



## D1.1 – ICD of the StL plant engineering

**Lead beneficiary: HyGear**

**Due date: 21 / 03 / 2024 (M4)**

**Actual submission date: 02 / 09 / 2024**

<b>Grant Agreement number</b>	GA 101122206
<b>Project acronym</b>	SUN-to-LIQUID II
<b>Project title</b>	SUNlight-to-LIQUID: Efficient solar thermochemical synthesis of liquid hydrocarbon fuels using tailored porous-structured materials and heat recuperation
<b>Type of action</b>	Research and Innovation (RIA)
<b>Start date of the project</b>	01/11/2023
<b>Duration</b>	48 months
<b>Project coordinator (organisation)</b>	Dr Andreas Sizmann (Bauhaus Luftfahrt)
<b>Phone</b>	+49-171-3373210
<b>E-mail</b>	contact@sun-to-liquid-2.eu
<b>Website</b>	<a href="http://sun-to-liquid-2.eu">sun-to-liquid-2.eu</a>



**Funded by  
the European Union**

**Project funded by**



Schweizerische Eidgenossenschaft  
Confédération suisse  
Confederazione Svizzera  
Confederaziun svizra

Swiss Confederation

Federal Department of Economic Affairs,  
Education and Research EAER  
**State Secretariat for Education,  
Research and Innovation SERI**

Funded by the European Union under GA 101122206. Views and opinions expressed are however those of the author(s) only and do not necessarily reflect those of the European Union. Neither the European Union nor the granting authority can be held responsible for them.

This work has received funding from the Swiss State Secretariat for Education, Research and Innovation (SERI).

## Document information

<b>Document Name</b>	D1.1 – ICD of the StL plant engineering
<b>Version</b>	VF
<b>Version Date</b>	02/09/2024
<b>Author</b>	Daan Kok (HyGear)
<b>Dissemination level</b>	Public

## Approvals

	<b>Full Name</b>	<b>Organisation</b>	<b>Date</b>
<b>Coordinator</b>	Andreas Sizmann	BHL	29/08/2024
<b>WP Leader</b>	Manuel Romero	IME	29/08/2024
<b>Task Leader</b>	Daan Kok	HyGear	29/08/2024
<b>Other (Quality)</b>	Julie Chupin	LUP	02/09/2024

## Documents history

<b>Version</b>	<b>Date</b>	<b>Modification</b>	<b>Name (Organisation)</b>
V6	09/07/2024	For final review by coordinator	D.Kok (HYG)
V6_Asi	12/08/2024	First review & Approval	A.Sizmann (BHL)
V7	16/08/2024	Final version for review	D.Kok (HYG)
V8	29/08/2024	Final version for submission	D.Kok (HYG)
VF	02/09/2024	Quality Check	J. Chupin (LUP)

## Distribution list

<b>Name</b>	<b>Organisation</b>
SUN-to-LIDUID II Consortium	N/A
Project Officer Luca Bondi	EC / CINEA

## Executive summary

The overall solar-to-fuel plant consists of several modules like solar field, flux measurement system, solar reactor, heat recovery system and gas-to-liquid (GtL) plant. During the development of the modules, it is important that all of them are well matched. The expected Process Flow Diagram (PFD), input and output data of all modules, input/out interfaces and plant specifications is herewith collected and documented in an interface control document (ICD), led by HYG in coordination IME (responsible for solar field), and DLR (for conceptual reactor design. On the basis from ICD, the corresponding on-site adaptations of the experimental facility will be performed to facilitate the smooth hosting of sub-systems (e.g. power supply needs, water supply needs, heat rejection/chiller, IT, gas supply and gas connections between systems, etc.).

### PROPRIETARY RIGHTS STATEMENT:

This document contains information, which is proprietary to the SUN-to-LIQUID II consortium. Neither this document nor the information contained herein shall be used, duplicated or communicated by any means to any third party, in whole or in parts, except with the priori written consent of the SUN-to-LIQUID II consortium. This restriction legend shall not be altered nor obliterated on or from this document.

# Table of contents

<b>Executive summary</b> .....	<b>3</b>
<b>1. Introduction</b> .....	<b>7</b>
<b>2. Solar field</b> .....	<b>8</b>
2.1. Heliostat solar field .....	8
2.2. Solar field input.....	9
2.3. Solar field output .....	9
<b>3. Solar receiver-reactor</b> .....	<b>11</b>
3.1. Solar reactor design.....	11
3.2. Dynamic behaviour: Cycle times .....	12
3.3. Operating temperatures and pressures.....	12
3.4. Solar-to-syngas efficiency .....	12
3.5. Input and output conditions .....	13
3.5.1. Upstream supply of gases to solar reactor.....	13
3.5.2. Flowrates: With heat recovery + active aperture shutter.....	14
3.5.3. Flowrates: Benchmark base situation without improvements .....	15
3.6. Downstream gas conditioning and gas analyser .....	15
<b>4. Gas-to-Liquid (GtL) plant</b> .....	<b>16</b>
4.1. GtL plant design.....	16
4.2. Input to GtL plant.....	17
4.2.1. Input from solar reactor to buffer tank .....	17
4.2.2. Input to the Fischer-Tropsch reactor .....	18
4.3. Output of GTL plant .....	19
<b>5. Equipment interfaces</b> .....	<b>20</b>
<b>6. Conclusion</b> .....	<b>21</b>
<b>7. References</b> .....	<b>22</b>

## List of figures

Figure 1: Process Flow Diagram (PFD) of the StL II plant adapted from the preceding StL II design as presented by Zoller et al., 2022. PFD showing the interfaces between the different subsystems. ....	7
Figure 2: Left: Aerial view of the heliostat field from the top of the solar tower. Right: Lateral view of a 3 m <sup>2</sup> heliostat with two rectilinear actuators.....	8
Figure 3: Lateral drawing of solar field reflecting distance between heliostat rows and position or focal point on tower top.....	9
Figure 4: Schematic overview of GtL plant.....	16

## List of tables

Table 1: Solar input and ambient conditions .....	9
Table 2: Solar field output / Solar reactor input .....	10
Table 3: Operating conditions solar reactor .....	12
Table 4: Solar-to-syngas efficiency .....	13
Table 5: Specification of supply gasses to solar reactor .....	14
Table 6: In- and output flowrates to be determined (tbd) – with heat recovery and active aperture shutter.....	14
Table 7: In- and output flowrates to be determined (tbd) - benchmark case without improvements .....	15
Table 8: Flowrates to be determined (tbd) to GtL reactor dependent if only H <sub>2</sub> O, only CO <sub>2</sub> or a mixture of H <sub>2</sub> O and CO <sub>2</sub> is supplied to the solar reactor. Excess reactants H <sub>2</sub> O and CO <sub>2</sub> not included. ....	18
Table 9: Specification of syngas at interface to GtL plant (prior to compression step). ....	18
Table 10: Required composition of syngas in buffer tank before entering the FT reactor .....	18
Table 11: Operating conditions of FT reactor .....	19
Table 12: Expected output of FT reactor based on constant input flow from buffer tank .....	19

# Glossary

Acronym	Meaning
<b>ICD</b>	Interface control document
<b>StL</b>	SUN-to-LIQUID
<b>GtL</b>	Gas-to-Liquid
<b>FT</b>	Fischer-Tropsch
<b>PFD</b>	Process Flow Diagram
<b>DNI</b>	Direct Normal Irradiance
<b>HTF</b>	Heat Transfer Fluid
<b>TES</b>	Thermal Energy Storage
<b>BHL</b>	Bauhaus Luftfahrt, SUN-to-LIQUID II Coordinator
<b>DLR</b>	Deutsches Zentrum für Luft- und Raumfahrt
<b>IME</b>	Fundación IMDEA Energía,
<b>HYG</b>	HyGear B.V.
<b>WP</b>	Work Package
<b>SoA</b>	State of Art

# 1.Introduction

This document is the interface control document (ICD) of the SUN-to-LIQUID II (StL II) plant. The document describes the input and output data of the different modules within the plant, as well as the different input/output interfaces and plant specifications.

The goal of the document is to use it as a basis for the redesign, on-site adaptations and optimization of the already existing experimental facility that was built as part of the preceding H2020 SUN-to-LIQUID project. With the ambitious goal to increase the solar reactor energy efficiency up to 15% or higher (compared with 4.1% in the preceding project), corresponding to an estimated production of 750 L syngas per sunny day, the operating conditions and in particular the expected in- and output volume streams of the various modules significantly changes. To make sure all the separately build and tested modules work together as one plant in the end it is of importance that the interfaces between the modules are perfectly aligned with each other.

Figure 1 illustrates the process flow diagram (under development) of the solar-to-fuel plant consisting out of a solar field with heliostats, the solar reactor at the top of the tower and the gas-to-liquid (GtL) unit. In short, a heliostat field concentrates the direct normal solar irradiation onto a solar reactor mounted on top of the solar tower. The solar reactor co-splits  $H_2O$  and  $CO_2$  and produces a specific mixture of  $H_2$  and  $CO$  (syngas), which in turn is processed to liquid hydrocarbon fuels using the FT-based GtL unit located next to the solar base. Here IME is responsible for the solar field, the gas and steam supply and the downstream gas analysis. DLR is responsible for the design and development of the solar reactor including the new developed integrated heat recovery system and lastly HyGear is responsible for the gas-to-liquid (GtL) plant.

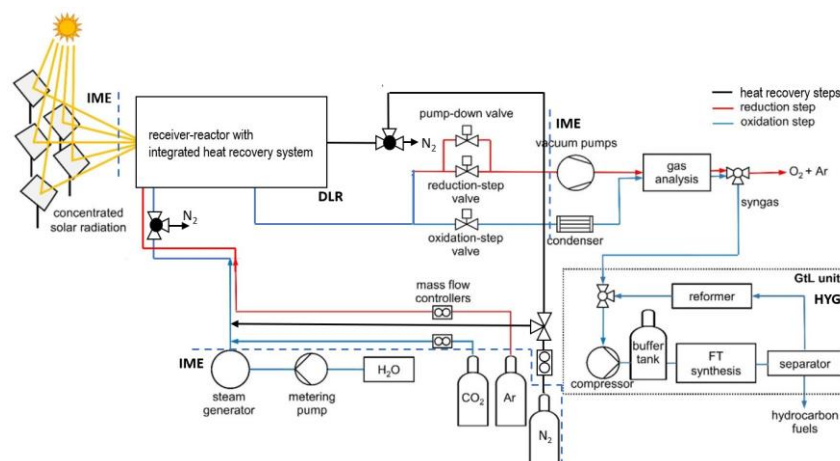


Figure 1: Process Flow Diagram (PFD) of the StL II plant adapted from the preceding StL II design as presented by Zoller et al., 2022. PFD showing the interfaces between the different subsystems.

In the remaining chapters of this document the different modules will be discussed further with a focus on the interfaces between each module. It must be noted that in this phase of the project the numbers given are subjected to further detailed engineering.

## 2. Solar field

The first module is the solar field designed and developed by IME.

### 2.1. Heliostat solar field

The heliostat field is shown in the photograph of [Figure 2](#) (left). It consists of 169 heliostats, 3 m<sup>2</sup> each, arranged in a 14-row cornfield layout with the mirrors curved at focal lengths of 20 m (rows 1-8) and 30 m (rows 9-14). The row and azimuthal spacing between the single facet heliostats are 2.25 and 2.60 m respectively ([Figure 3](#)), resulting in 47% land use, and the distance from the tower to the first row of heliostats is only 4 m.



Figure 2: Left: Aerial view of the heliostat field from the top of the solar tower. Right: Lateral view of a 3 m<sup>2</sup> heliostat with two rectilinear actuators.

Each heliostat ([Figure 2](#), right) is mounted on a 1.4 m-height pedestal pole and tracks the sun according to a tilt-roll or fixed horizontal tracking with the help of two rectilinear actuators having a roll angle range  $\pm 100^\circ$ , elevation angle range  $20\text{-}90^\circ$  ( $90^\circ$  corresponding to the horizontal stow position facing to zenith), with tracking accuracy  $< 0.1^\circ$ . Cold mechanical bending was applied to 3 mm-thick rectangular mirrors (dimensions 1605x1900x3 mm, total reflectivity 94.3%), bonded to a metallic frame and pre-conformed by gravity sagging onto a master model to obtain a spherical curvature. The mean beam quality, excluding sunshape, is 2.5 mrad. Based on ray-tracing analysis for spring equinox, summer, and winter solstice, this facility may reach at design point solar noon a solar radiative power of about 250 kW, of which at least 50 kW are incident within a 16-cm dia. circular target on top of the solar tower throughout the entire year. The optical efficiency  $\eta_{\text{optical}}$  can reach values exceeding 70% provided radiation spillage is collected and used (Romero, González-Aguilar and Luque, 2017).

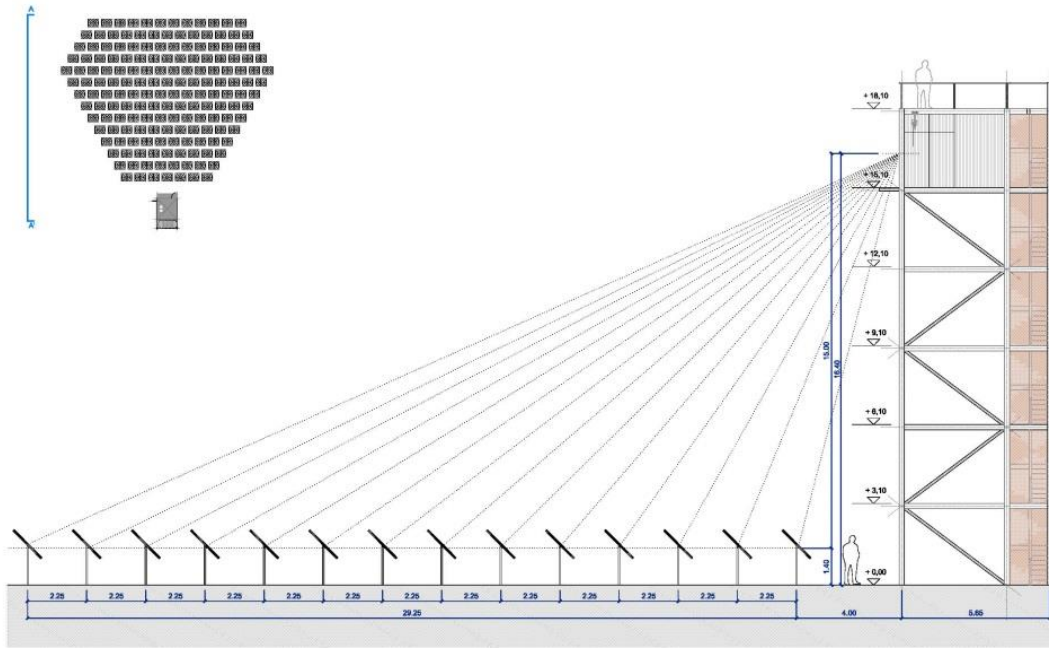


Figure 3: Lateral drawing of solar field reflecting distance between heliostat rows and position of focal point on tower top.

## 2.2. Solar field input

The input parameters of the solar field, mainly specified as the amount of solar radiation received, is critical for the further design and optimization of the solar-to-fuel plant. The parameters listed in Table 1 are obtained from on-site meteo station and solar tracker with pyrheliometer.

Table 1: Solar input and ambient conditions

	<i>Minimum</i>	<i>Nominal</i>	<i>Maximum</i>
<i>DNI (Direct Normal Irradiance (W/m<sup>2</sup>))</i>	300	800	1000
<i>Wind velocity (m/s)</i>	0	4	10
<i>Ambient temperature (°C)</i>	-10	20	45

## 2.3. Solar field output

The output parameters of the solar field onto the solar reactor are summarized in Table 2. Here is the interface between the solar field and the solar reactor. The given values are under the assumption that the solar reactor is mounted on top of the solar tower at an optical height of 15m, tilted 40° downward relative to the horizontal plane, and aimed at the power-weighted centre of the heliostat field.

From the table can be seen that a nominal output of the solar field (or input for the solar reactor) of 50 kW is targeted during the reduction step of the solar reactor. This value can be permanently guaranteed due to the available total output of the heliostat field of 250 kW. Tests at reduced (20 kW) and increased power (70 kW) are planned to characterize the reactor and the overall system.

Table 2: Solar field output / Solar reactor input

	<i>Minimum</i>	<i>Nominal</i>	<i>Maximum</i>
<i>Power input during reduction (kW)</i>	20	50	70
<i>Power input during oxidation (kW)</i>	0	0	0
<i>Average Irradiance (kW/m<sup>2</sup>)</i>	1000	2500	3500
<i>Peak Irradiance (kW/m<sup>2</sup>)</i>	-	-	4000
<i>Ramp during heating (kW/min)</i>		5	70
<i>N° hours nominal around solar noon</i>	5 (winter)	6	7 (summer)

A risk is to be noted here that the given values for the power and irradiance come with an uncertainty of +/- 10 to 20% as these values are highly depending on the flux measurement system that will be further developed and implemented at a later stage of the project.

## 3. Solar receiver-reactor

The second module is the solar receiver-reactor designed by DLR. Within the SUN-to-LIQUID II project the goal is to further optimize the solar reactor by various different ways, with the biggest improvement being the integration of a heat recovery system. In this section the input and output parameters of the solar reactor will be discussed, which are in particular relevant for the operation of the downstream GtL plant.

### 3.1. Solar reactor design

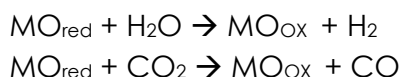
Figure 1 shows a basic schematic of the solar reactor design indicating its inputs and outputs, which will be detailed in the next sections. In short, in the reactor H<sub>2</sub>O and CO<sub>2</sub> are thermochemically converted into H<sub>2</sub> and CO or also called 'syngas'. This product gas is further processed in the downstream GtL module where the gas is converted to liquid hydrocarbons via Fischer-Tropsch (FT) synthesis.

The splitting of H<sub>2</sub>O and CO<sub>2</sub> in combination with the integrated heat recovery system will be a four-steps cycle - each step with different output and input parameters. Therefore, it is of importance to first describe the relevant steps:

- 1) Reduction step:** The cavity receiver containing a redox material structure is in this step directly exposed to concentrated solar radiation from the solar field. The heat drives the endothermic chemical reduction step where the metal oxide (MO<sub>OX</sub>) is reduced to a lower-valence metal oxide (MO<sub>red</sub>) and O<sub>2</sub> is released. This step is operated under vacuum.



- 2) Heat extraction step:** An inert gas as heat transfer fluid (HTF) is used to extract heat from the solar reactor which will be stored in a Thermal Energy Storage (TES). The solar reactor cools down until a temperature is reached at which the oxidation step can start
- 3) Oxidation step:** The reactants H<sub>2</sub>O and CO<sub>2</sub> in a certain ratio will be supplied to the solar reactor, resulting in re-oxidation of the reduced metal oxide and the production of CO and H<sub>2</sub> according to reactions given below. The oxidation step is exothermic and the cavity is not exposed to concentrated solar radiation. The product stream of H<sub>2</sub> and CO, syngas, is streaming out of the reactor.



- 4) Heat recuperation step:** Inert gas as heat transfer fluid (HTF) is now used to heat up the solar reactor as much as possible using the heat stored in the TES in the heat extraction step.

### 3.2. Dynamic behaviour: Cycle times

Each step will happen in series and take a certain amount of time. Therefore, the product stream of the reactor, syngas, is an intermittent flow going to the downstream GtL plant. The cycle times are therefore important for the sizing of the buffer and the buffering strategy of the GtL plant in order to continuously operate the Fischer-Tropsch reactor. It shall be noted that the cycle times will be based on model predictions and are subjected to detailed engineering at a later stage in the project.

In the preceding project H2020 SUN-to-LIQUID the cycle consisted only out of a reduction and oxidation step with passive cooling in between and no further heat recovery. This case will also be tested during SUN-to-LIQUID II project for benchmark purposes.

### 3.3. Operating temperatures and pressures

Nominal operating temperatures and pressures of the solar reactor are summarized in Table 3. The values are derived from Zoller et al. (2022).

Table 3: Operating conditions solar reactor

	Unit	Value
Reduction start temperature	°C	700 *
Reduction end temperature	°C	1500
Oxidation start temperature	°C	900
Oxidation end temperature	°C	700
Reactor pressure during reduction	mbar	26-100
Reactor pressure during oxidation	-	Atmospheric
Reactor pressure during heat extraction/recuperation	-	Atmospheric

\* It is expected that with the integration of the heat recovery system the reduction could start at somewhat higher temperatures.

### 3.4. Solar-to-syngas efficiency

The solar-to-syngas efficiency is an important parameter used in the calculations of the in- and output flowrates used further in this report. The solar-to-syngas energy conversion efficiency  $\eta_{\text{solar-to-syngas}}$  is defined as the ratio of the higher heating value of the syngas produced over the cycle to the sum of solar radiative power input  $Q_{\text{solar}}$  and other energy inputs (e.g. energy inputs associated with vacuum pumping).

$$\eta_{\text{solar-to-syngas}} = \frac{Q_{\text{syngas}}}{Q_{\text{input}}}$$

With the integration of the heat recovery system, advanced redox structures and an active aperture shutter a solar-to-syngas efficiency of 15% is expected. To be able to make the comparison with and without heat recovery and active aperture shutter both cases will be tested during the SUN-to-Liquid II project. Each case results in

significant different in- and output flowrates for which the solar reactor and GtL plant needs to be designed for.

Table 4: Solar-to-syngas efficiency

	<i>Operating case</i>	
	<i>Reference SoA RPC</i>	<i>With 3D printed structures + heat recovery + active aperture shutter</i>
<i>Solar-to-syngas efficiency (%)</i>	5	15

### 3.5. Input and output conditions

The input and output conditions will depend on the receiver-reactor design and the operational strategy. In order to quantify the different flow rates, a plant model is under development that allows to tailor design and operational parameters for optimal performance. The flowrates that will be determined by this model will be the base for the layout and construction of the plant modules. First in section 3.5.1 the specifications of the gases to be supplied to the reactor are given, being the interface between IME and DLR. In section 3.5.2. the different in- and output parameters for the case with heat recovery and active aperture shutter are presented (resulting in the highest flowrates). In section 3.5.3 the parameters for the benchmark case without the improvements are presented (resulting in the lowest flowrates). Ranges for the parameters in both tables can be provided, once the optimal values and uncertainties are determined by the model.

#### 3.5.1. Upstream supply of gases to solar reactor

IME, as solar field host, is responsible for the supply of the different gases to the solar reactor designed by DLR. Table 5 describes the specification (pressure, temperature) of the gases to be supplied by IME to the solar reactor. The required parameters are indicated in Table 6 and Table 7.

Table 5: Specification of supply gasses to solar reactor

Gas	Type	Conditions	Description
H <sub>2</sub> O	Reactant	T: 250 °C	Water (in the form of steam) and CO <sub>2</sub> (supplied from bottles) are consumed as reactants in the oxidation step. The H <sub>2</sub> O:CO <sub>2</sub> ratio must be adjustable in order to get the right quality of syngas produced. For the calculations a ratio of 2:1 is used.
		P: tbd	
CO <sub>2</sub>	Reactant	T: 250 °C	
		P: tbd	
Ar	Inert	T: 20 °C	Argon coming from bottles will be needed for the internal cooling of the reactor window and to keep the window clean of depositions.
		P: 6 bara	
N <sub>2</sub>	Sweep gas / HTF	T: 20 °C	Nitrogen coming from bottles is used as sweep gas and Heat Transfer Fluid (HTF) for the thermal energy storage system.
		P: 6 bara	

### 3.5.2. Flowrates: With heat recovery + active aperture shutter

Table 6 gives an overview of the expected in- and output parameters. Values will be determined once the corresponding model is finalized.

Table 6: In- and output flowrates to be determined (tbd) – with heat recovery and active aperture shutter

	Phase			
	<i>Pre-Heating (recuperation)</i>	<i>Reduction</i>	<i>Active cooling (heat recovery)</i>	<i>Oxidation</i>
<b>Input (sl/min)</b>				
H <sub>2</sub> O	0	0	0	tbd
CO <sub>2</sub>	0	0	0	tbd
Ar	tbd	tbd	0	0
N <sub>2</sub>	tbd	0	tbd	tbd
<b>Output (sl/min)</b>				
H <sub>2</sub> O	0	0	0	tbd
H <sub>2</sub>	0	0	0	tbd
CO	0	0	0	tbd
CO <sub>2</sub>	0	0	0	tbd
Ar	0	tbd	0	0
N <sub>2</sub>	tbd	0	tbd	tbd
O <sub>2</sub>	0	tbd	0	0

### 3.5.3. Flowrates: Benchmark base situation without improvements

For benchmarking, it is planned to operate the receiver-reactor similarly to the one in the preceding project SUN-to-LIQUID. As a result, the phases and flow rates for the benchmarking campaign will have to be adapted. Table 7 gives an overview of the expected in- and output parameters based on the benchmark SoA efficiency of 5%.

Table 7: In- and output flowrates to be determined (tbd) - benchmark case without improvements

	Phase		
	Reduction	Passive cooling	Oxidation
<b>Input (sl/min)</b>			
H <sub>2</sub> O	0	0	tbd
CO <sub>2</sub>	0	0	tbd
Ar	tbd	0	0
N <sub>2</sub>	0	0	0
<b>Output (sl/min)</b>			
H <sub>2</sub> O	0	0	tbd
H <sub>2</sub>	0	0	tbd
CO	0	0	tbd
CO <sub>2</sub>	0	0	tbd
Ar	tbd	0	0
N <sub>2</sub>	0	0	0
O <sub>2</sub>	tbd	0	tbd

### 3.6. Downstream gas conditioning and gas analyser

The two outlet streams first will be conditioned and passed through a gas analyser (scope of IME). As can be seen from the Table 3 the reduction step happens under vacuum conditions for better performance at lower oxygen partial pressures. Hence, during reduction step, the outlet O<sub>2</sub> stream is released using vacuum pumps. The oxidation step happens at atmospheric conditions. Hence the outlet syngas stream during the oxidation steps goes through a condenser to remove unreacted water before going to the gas analyser and subsequently to the StL plant.

The gas analysis is performed by a gas chromatograph and two gas analysers Calomat 6 and Ultramat 23, able to measure H<sub>2</sub>, O<sub>2</sub>, CO and CO<sub>2</sub>. For sizing of the vacuum pumps and condenser flow rate Table 6 and Table 7 for respectively the 5% and 15% efficiency test case will have to be considered.

## 4. Gas-to-Liquid (GtL) plant

The third and last module is the gas-to-liquid (GtL) plant where the solar syngas is further processed and converted to liquid fuels. Due to the significantly higher reactor efficiencies and the coupling with the energy storage system the existing GtL conversion unit will require the redesign of several parts of the system and specifically requires optimization of the buffer tank to accommodate for the larger syngas flowrates received from the solar reactor.

### 4.1. GtL plant design

The GtL plant basically consists out of 3 modules as schematically presented in Figure 4, being the compression and buffer module, the Fischer-Tropsch reactor and product separation module and the steam reformer which are further described below. By choosing the right buffer size and strategy the goal is to be able to separately run the GtL plant and the solar reactor to have continuous production of kerosene and increase the product yield.

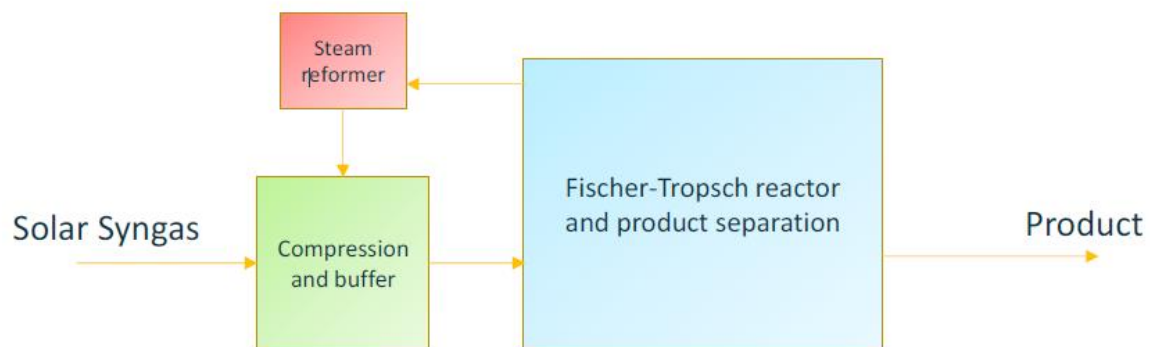


Figure 4: Schematic overview of GtL plant

#### Compression and buffer

First is the syngas received from the solar reactor is compressed and stored in a buffer vessel. The buffer tank is there to create a situation that the FT reactor can run independent in time and operation of the solar reactor (i.e. when no sunlight is available). Based on the syngas flowrates and cycle times the pressure in the buffer tank and the buffer strategy is to be optimized.

The buffer tank incorporates a sampling port for analysis gas composition (and determine the ratio H<sub>2</sub>:CO)

#### Fischer Tropsch reactor and production separation

In the Fischer-Tropsch module the syngas mixture is converted into a mixture of gaseous, liquid and solid hydrocarbons (waxes) at a pressure of about 20 barg and 210°C. Downstream of the

reactor is a system for separation of waxes, liquid hydrocarbons and the gaseous components which are small hydrocarbons (C1-C6) and left over CO, H<sub>2</sub> and CO<sub>2</sub>.

### **Steam reformer**

In the steam reformer module, the leftover gaseous components from the FT reactor will be recycled in the steam reactor. The gaseous components are mixed with steam, heated to 700 °C and fed to a steam reformer catalyst. Here CH<sub>4</sub> and the higher hydrocarbons (ethane, propane, etc.) will react with steam to H<sub>2</sub> and CO again. Also, the CO<sub>2</sub> reacts here to CO by the reversed water gas shift reaction. The product gases are cooled down and mixed again with the syngas from the solar reactor.

## 4.2. Input to GtL plant

By using a buffer tank in between the solar reactor and the FT reactor there is a possibility to operate the FT reactor independently of the solar reactor. The decoupling offers the possibility to optimize the GtL plant separately from the solar reactor. In principle by operating the GtL plant around the clock, a day-and-night production of solar fuels can be realized. Therefore, in order to specify the input conditions a distinction is made between the input from the solar reactor to the buffer tank and from the buffer tank to the FT reactor.

### 4.2.1. Input from solar reactor to buffer tank

Based on the tables given in section 3.5.2 and section 3.5.3 the expected flowrates of the syngas arriving at the interface of the GtL plant going to the buffer tank can be derived. Dependent on the mode of operation of the solar reactor (e.g. if only CO<sub>2</sub>, only H<sub>2</sub>O or a mix of H<sub>2</sub>O and CO<sub>2</sub> is supplied to the solar reactor) the expected flowrates to the GtL are summarized in Table 8. Pressure and temperature of the syngas at the interface to the GtL plant (hence after conditioning and going through the gas analyser, but before compression step in GtL plant) is presented in Table 9. Ratio H<sub>2</sub>:CO in the incoming stream from the reactor can change in order to keep a value of approx. two in the buffer tank.

All the excess H<sub>2</sub>O is condensed out of the syngas by the condenser before it arrives at the GtL interface.

Table 8: Flowrates to be determined (tbd) to GTL reactor dependent if only H<sub>2</sub>O, only CO<sub>2</sub> or a mixture of H<sub>2</sub>O and CO<sub>2</sub> is supplied to the solar reactor. Excess reactants H<sub>2</sub>O and CO<sub>2</sub> not included.

	<b>Flowrate (sL/min)(min/nom/max)</b>	
	<i>Without heat recovery</i>	<i>With heat recovery + active aperture shutter</i>
H <sub>2</sub>	tbd	tbd
CO	tbd	tbd
H <sub>2</sub> + CO	tbd	tbd

Table 9: Specification of syngas at interface to GTL plant (prior to compression step).

	<i>Unit</i>	<i>Value</i>
<i>Syngas temperature</i>	°C	~10 - 40
<i>Syngas pressure</i>	barg	Atmospheric

It shall be noted that the recycle stream from the reformer back to the buffer tank will be mixed with the syngas stream from the solar reactor before both streams enter the compression step. The recycle stream shall have the same specifications as mentioned in Table 9. The flowrate and composition of the recycle stream are to be determined, but these details are not relevant for this interface document.

#### 4.2.2. Input to the Fischer-Tropsch reactor

The FT reactor requires a stable and continuous input from the buffer tank for smooth operation. Only when the gas composition in the buffer tank is according specifications the FT can start operation. The specification of the composition of the syngas going into the FT reactor is given in Table 10. The operating conditions of the FT reactor are given in Table 11. The temperature and pressure given in this table is coming from the FT reactor that was designed for the preceding SUN-to-LIQUID project and will be optimized during the redesign of the FT reactor.

Dependent on the measured composition in the buffer tank the supply of H<sub>2</sub>O and/or CO<sub>2</sub> to the solar reactor can be adjusted. When the composition in the buffer tank is out of spec the gas will be vented or, as backup scenario, H<sub>2</sub> and CO bottles will be available to ensure right composition in the buffer tank is maintained.

Table 10: Required composition of syngas in buffer tank before entering the FT reactor

Gas	Composition
H <sub>2</sub>	>1.2 * CO
CO	>30%
CO <sub>2</sub>	Acts as inert
CH <sub>4</sub>	Acts as inert
Inert gasses (N <sub>2</sub> or Ar)	Acts as inert

Table 11: Operating conditions of FT reactor

	<i>Unit</i>	<i>Value</i>
<i>Operating pressure FT reactor</i>	<i>barg</i>	<i>20</i>
<i>Operating temperature FT reactor</i>	<i>°C</i>	<i>200-220</i>
<i>Flowrate to FT reactor</i>	<i>sL/min</i>	<i>7 (2.4 slm CO)</i>

### 4.3. Output of GTL plant

In the Fischer-Tropsch reactor H<sub>2</sub> and CO are converted into hydrocarbons and water. The liquid hydrocarbons and waxes are separated in the product separation section. The separated gaseous species – methane up to butane – are recycled to the stream reforming module. Part of the separated waxes will be converted in a new developed reactor to Kerosene. Table 12 summarized the expected outputs of waxes and kerosene based on a constant flow of syngas to the FT reactor as specified in Table 11.

Table 12: Expected output of FT reactor based on constant input flow from buffer tank

	<i>Unit</i>	<i>Value</i>
<i>Expected wax production</i>	<i>g/day</i>	<i>550 (based on 24h/day operation)</i>
<i>Expected kerosene production *</i>	<i>g/day</i>	<i>440 (based on 24h/day operation)</i>

\*The given value for kerosene production is a hypothetical value based on literature. The value is subjected to detailed engineering as the reactor is still in development.

## 5. Equipment interfaces

Each subsystem of the StLII plant has their own in- and outlet ports. For adequate integration of the subsystems, the exact connection sizes need to be shared between the partners once available. At this stage of the project the parameters and values are unknown and shall be updated at a later stage during the project.

## 6. Conclusion

The overall solar-to-fuel plant consists of several modules like solar field, flux measurement system, solar reactor, heat recovery system and GtL plant. During the development of the modules, it is important that all of them are well matched. The expected PFD (Process Flow Diagram), input and output data of all modules, input/out interfaces and plant specifications is herewith collected and documented in an interface control document (ICD). On the basis from ICD, the corresponding on-site adaptations of the experimental facility will be performed to facilitate the smooth hosting of sub-systems (e.g. power supply needs, water supply needs, heat rejection/chiller, IT, gas supply and gas connections between systems, etc.).

As detailed engineering is still to be carried out the parameters given in this table are subjected to changes.

## 7. References

*M. Romero, J. González-Aguilar and S. Luque (2017). Ultra-modular 500m2 heliostat field for high flux/high temperature solar-driven processes. In AIP Conference Proceedings. 1850 (1). AIP Publishing. 10.1063/1.4984387.*

*S. Zoller, E. Koepf, D. Nizamian, M. Stephan, A. Patané, P. Haueter, M. Romero, J. González-Aguilar, D. Lieftink, E. de Wit, S. Brendelberger, A. Sizmann, A. Steinfeld: A solar tower fuel plant for the thermochemical production of kerosene from H<sub>2</sub>O and CO<sub>2</sub>, Joule vol.6 (7), 2022, doi.org/10.1016/j.joule.2022.06.012*